QUALITY TECHNOLOGY & QUANTITATIVE MANAGEMENT
https://doi.org/10.1080/16843703.2022.2071526

The alpha power Weibull transformation distribution applied to describe the behavior of electronic devices under voltage stress profile

Luis Carlos Méndez-González, Luis Alberto Rodríguez-Picón, Ivan Juan Carlos Pérez-Olguin, Luis Asunción Pérez-Domínguez and David Luviano Cruz

Department of Industrial Engineering and Manufacturing, Institute of Engineering and Technology, Universidad Autónoma de Ciudad Juárez, Ciudad Juárez, México

ABSTRACT

This paper presents a life-stress methodology that models the failure rate in the form of a bathtub curve. The model consists of the Alpha Power Transformation (APT), which adds an extra parameter to the probability distributions to achieve better flexibility in the representation in the data analysis. To build the life–stress relationship, the APT is combined with the Weibull Distribution (WD) and the Inverse Power Law (IPL) as a stress model to relate the data from the accelerated life tests (ALT), thus presenting the APTW-IPL. Statistical properties of the APTW-IPL are analyzed and discussed. For the parameter estimation of APTW-IPL, the Maximum Likelihood Estimator was used. On the other hand, to test the efficacy of the APTW-IPL, the model is compared with other methodologies that describe the behavior of the bathtub curve in two case studies related to determining the behavior of electronic devices that were subjected to ALT. The results show that the APTW-IPL can be a good option for reliability analysis in electronic devices. It represents the failure times in the form of a bathtub curve, the value of MTTF, and fitting the distribution to the case study data.

ARTICLE HISTORY
Accepted 9 April 2022

KEYWORDS
Alpha power Weibull distribution; accelerated life testing; bathtub failure rate; electronic devices; inverse power law

1. Introduction

Reliability engineering has become a powerful tool to determine the behavior of devices over time. One of the most ingrained concepts within reliability is the description of failure rate times through the bathtub curve. In the case of complex composition systems such as electronic devices (ED), the failure rates exhibited by this class of components are non-monotonic; this is usually taking the form of increased failure rate early (wear-in) and late decreasing failure rate (wear-out) in the component lifetime (Bebbington et al., 2007). Nevertheless, suppose the behavior of ED is represented under some classical probability distribution such as the WD (which would be the first choice for its negatively and positively skewed density shape). In that case, it shows that the failure rate behaves in a monotonic way, thus breaking the principle of the bathtub shape. Consequently, the WD cannot provide an excellent fit to lifetime datasets with bathtub-shaped or upside-down bathtub-shaped (unimodal) failure rates, mainly when the ED is under a reliability analysis.

Nowadays, WD modifications have been proposed through diverse mathematical techniques to ensure that the behavior described is closest to the bathtub shape. For example, Mann et al. (1974) proposed the mixture of the WD with other distributions to obtain a better fit of the data obtained

CONTACT Luis Carlos Méndez-González luis.mendez@uacj.mx Department of Industrial Engineering and Manufacturing, Institute of Engineering and Technology, Universidad Autónoma de Ciudad Juárez, Ciudad Juárez, Chihuahua 32310, México

© 2022 International Chinese Association of Quantitative Management

through accelerated life testing (ALT). He et al. (2019) described a method for detecting the inflection point of a bathtub curve for ED, which indicates the time when the failure rate becomes stable. The method was proposed via statistics index, which is used in a control chart to calculate the burn-in time and the warranty time of the ED under production. Hjorth (1980) proposed a general methodology for the design of distributions capable of modeling bathtub curves through three parameters (one of scale and two of shape). This methodology is less restrictive than the distributions of one and two parameters such as WD. Xie and Lai (1996) proposed the methodology of additive distributions through the sum of the hazard rate functions with increasing rate and hazard rate function with the decreasing rate. With this methodology, the Additive Weibull distribution (AWD) was proposed. Xie et al. (2002) proposed a Flexible WD based on Hjorth's methodology, obtaining greater flexibility in the representation of the bathtub curve since the confidence intervals for the shape parameter and the joint confidence regions for the two parameters have a closed-form which modeling of infant failure rate is put forward first. Bebbington et al. (2007) introduced a flexible WD extension based on a two-parameter ageing on the model proposed by Gurvich et al. (1997) with the difference that $F(t)$ is not a monotonic function of t. Lu and Chiang (2018) modified the WD to make the failure rate more flexible than the modified WD through a zero-truncated power series distribution.

Other methodologies have proposed hybrid distributions, which consist of the combination of two distributions in order to obtain the mixed benefits of the distributions. Lai et al. (2016) introduced a new parameterization with which it is possible to represent the failure rate in the form of a bathtub curve through a portion of the beta distribution (BD). The distribution has a finite range, which is appropriate when there is a maximum possible lifetime and a common scenario when additional failure modes fail after a particular time. Lee et al. (2007); Silva et al. (2010) proposed and analyzed the benefits of mixing the BD distribution with the WD, obtaining a distribution with two shape and two-scale parameters they called the Beta-Weibull Distribution (BW). The main problem with this distribution is that the failure rate function cannot be expressed explicitly. Ali et al. (2019) and Méndez-González et al. (2017) demonstrated the use of BW to describe the behavior of ED when subjected to ALT and analyzed with IPL. The combination of both models forms a life–stress relationship in which the effects of the parameters on the life of the device were determined. Other authors like Ali et al. (2020), Méndez-González et al. (2019), and Nadarajah et al. (2013) analyzed and applied the generalization of the WD based on the introduction of an exponentialization of the failure rate function; the advantage of this distribution is that it can be adjusted to a large amount of data. The problem in this distribution is that if t is minimal and scarce, the failure rate tends to be a WD, which may not be a good choice if the data comes from an ALT where the information is short and sometimes censored. In the models mentioned above, the use of the beta, exponential and additive families show an alternative but with certain deficiencies for the bathtub curve fit; since these models focus more on representing the non-monotone behavior of the device under analysis.

In recent years, a new family of distributions is being used to analyze bathtub failure rates; this family is called the APT, which provides a better fitting and flexibility to analyze positive real data from a reliability test. Lehmann (1953) proposed a family based on the cumulative function considering $\mathbb{F}(x;\alpha) = f(x)^{\alpha}$, which was the basis for Durrans (1992) to propose the APT taking into consideration α^{+}. Mahdavi and Kundu (2017) introduced the APT by adding a new parameter to the exponential family of distributions; this new parameter incorporated skewness to a family of distribution functions. This proposed model provides a better fit than existing models and retains similar properties to that of the Gamma and Weibull families. Gamma and Weibull families. Ahmad et al. (2018), Mead et al. (2019), and Zaizai (2019) and NIU proposed statistical properties of the APT. On the other hand, Dey et al. (2017) proposed combining APT with WD, calling it Alpha Power Weibull Transformation (APTW); this distribution can model failure rate functions with the following forms depending on its shape parameters: monotonically increasing, decreasing, constant, concave-convex, and reverse J-shaped hazard rates. Nassar, Afify et al. (2018) and Nassar

et al. (2017) define properties and different methods of estimation of the APTW. Elbatal et al. (2018) proposed a three-parameter new alpha power transformed WD with properties to censoring data. Other APTW applications can be found in Basheer (2019), Nassar, Alzaatreh et al. (2018), and Ramadan and Magdy (2018).

All the bathtub curve methodologies presented above have been proposed from the data from simulation or an ideal perspective. So, in a practical sense, it can be unattractive for reliability engineers who wish to apply new methodologies if the models do not offer a life-stress methodology centered on the reality of the devices. On the other hand, He et al. (2016) establish that the models that describe the behavior of the faults in the shape of a bathtub curve are more focused on performance at the part level. However, at the production level, they have not delved into aspects such as describing the quality data and other characteristics inherent to the product when it is in the mass production stage.

Therefore, given the above, it is crucial to building a model capable of obtaining electronic product reliability and quality metrics through a life–stress relationship. This research aims to present a model using the APTW and the IPL, with which the failure rates of EDs are described when they are subjected to ALT with voltage stresses; this model is called APTW-IPL. For the practitioners, a physical description of the parameters of the proposed model is presented. The MLE is used to estimate the related parameters of APTW-IPL. We illustrate the importance of the proposed life–stress relationship over the AWD, BW, Beta Generalized Weibull Distribution (BGWD), Generalized Exponential Distribution (GED), and Exponentiated-Weibull (EXW), all distributions combined with the IPL. To determine the efficiency of the proposed model, the APTW-IPL is tested in two case studies related to ED, where the data were obtained from an ALT. The comparative analyses in the case studies include verifying the data in the form of a bathtub curve. This analysis is performed through the Total Time on Test (TTT) plot, the Mean Time to Failure (MTTF), the adjustment of the data, and the behavior graphs of the devices in operating voltage. The devices considered for the analysis are DC micromotor (DCMM), one of the most critical components of a medical device used to detect internal injuries. The other device is a Linear Variable Differential Transformer (LVDT) used in test equipment which verifies a turbo system in the automotive sector

Finally, this paper is organized as follows. Section 2 presents the APTW model background. Section 3 presents the construction of the life-stress model. Section 4 presents the statistical properties of APTW-IPL. Section 5 presents a proposal modeling of the APTW-IPL in time-varying stress focused on ED. Section 6 presents the likelihood function to calculate the parameters proposed in section 3. Section 7 presents the cases of study of the paper and discussion. The last section provides concluding remarks and future work about the proposed model

2. APTW model background

Let $G(x)$ be the CDF of a continuous variable X, then the APT of $G(x)$ for x is defined as follow:

$$F_{APT}(x) = \frac{\alpha^{G(x)} - 1}{\alpha - 1} \, if \, \alpha > 0, \alpha \neq 1 \tag{1}$$

Based on Mahdavi and Kundu (2017), if on Equation (1) $G(x)$ is a continuous distribution with a probability density function (PDF) $g(x)$, then $F_{APT}(x)$ is also an absolute continuous distribution function with the PDF:

$$f_{APT}(x) = \left(\frac{log(\alpha)}{\alpha - 1}\right)\left(g(x)\alpha^{G(x)}\right) if \, \alpha > 0, \alpha \neq 1 \tag{2}$$

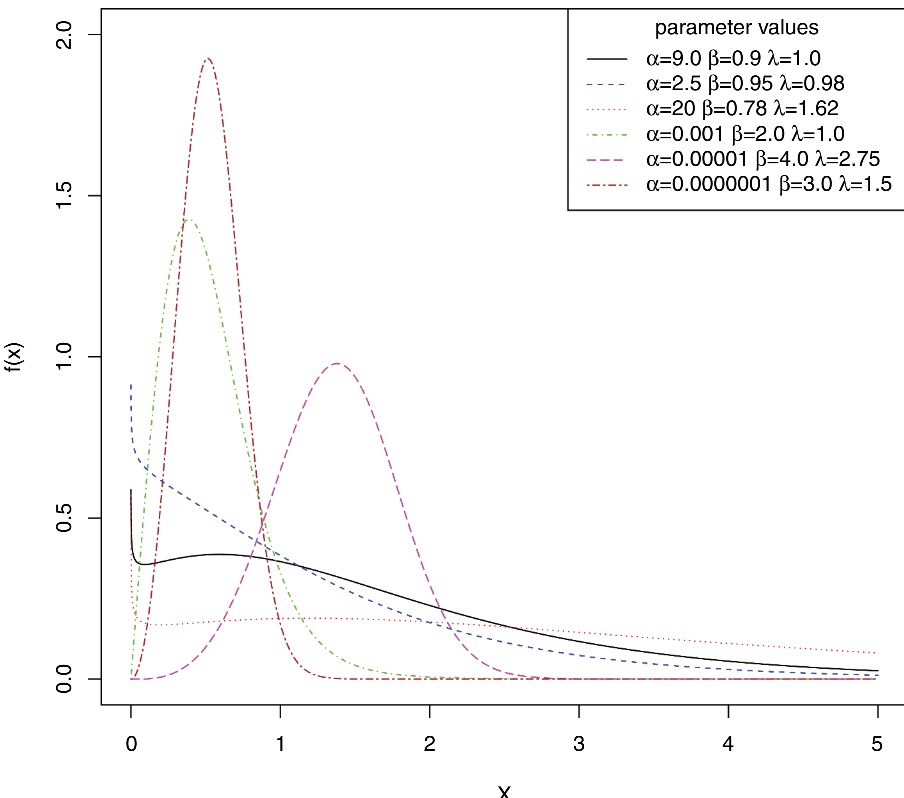

Figure 1. PDF for some APTW-derived parameter values.

By setting $g(x)$ the Probability Density Function (PDF) of WD with scale parameter λ, a shape parameter β, and $G(X)$ as the CDF of WD and following Equation (2) the PDF of the APTW is described as follow:

$$f_{APTW}(x) = \left[\frac{log(\alpha)}{\alpha - 1}\right] \frac{\beta}{\lambda} \left(\frac{x}{\lambda}\right)^{\beta-1} e^{-\left(\frac{x}{\lambda}\right)^{\beta}} \alpha^{\left(1-e^{-\left(\frac{x}{\lambda}\right)^{\beta}}\right)} \tag{3}$$

$f_{APTW}(x)$ presented in (3) must follow $x, \alpha, \beta, \lambda > 0, \alpha \neq 1$. In Figure 1, it is presented a comparison of different PDF for the f_{APTW} expressed by (3). Additionally, in Figure 2 different shapes of the failure rate derived from (3) are showed.

In the following section, we use the APTW described in Eq uation (3) and the IPL to obtain the life–stress relationship distribution, which describes the behavior of devices under a voltage stress scenario; the presented model can be valid for any ED under a voltage stress scenario.

3. Life–stress model

To know the behavior of ED under-voltage scenarios, the IPL is used, which is described as:

$$L = \frac{1}{\omega v^{\gamma}} \tag{4}$$

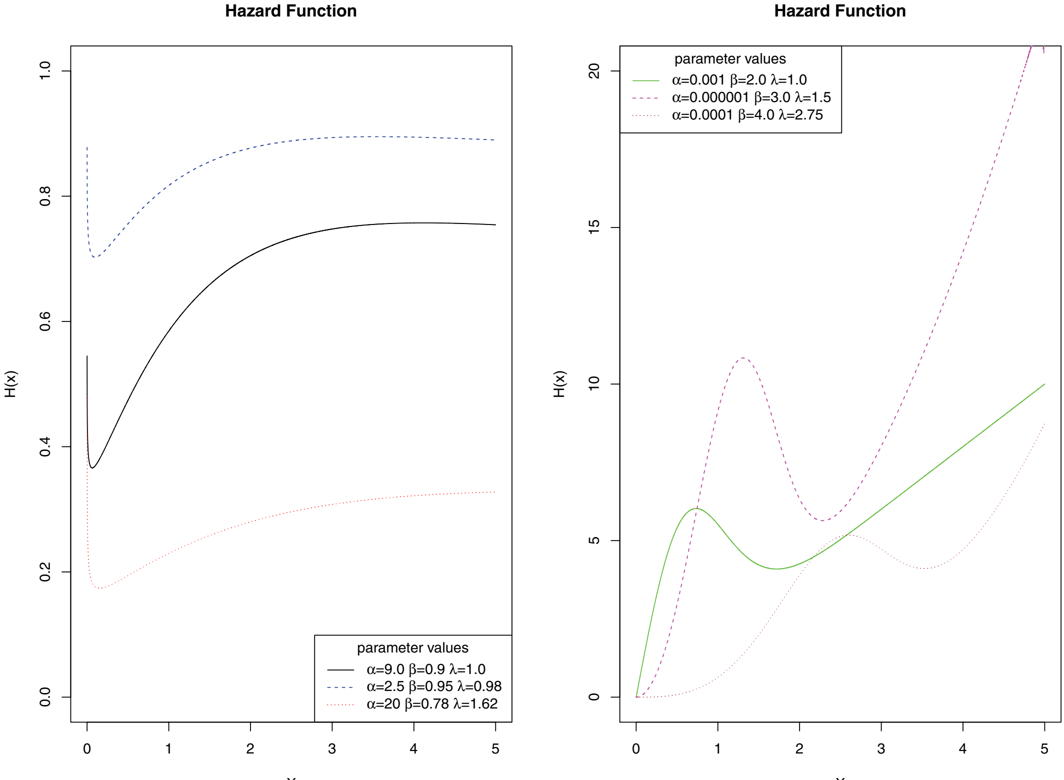

Figure 2. Hazard shape for some APTW derived parameter values.

Where parameter $\omega > 0$ represents a characteristic associated with material properties and product design. Parameter $\gamma > 0$ measures the effect of the applied stress in the device's behavior and lifetime. Finally, parameter $v > 0$ represents the voltage level applied in the piece under an ALT.

To build the life-stress model, it is necessary to follow the assumption of this type of relationship, which indicates that the shape parameters are maintained during the test times, and the scale parameter changes over time. Therefore, when taking the scale parameter in Equation (3) and replacing it with the IPL model presented in Equation (4), the following is obtained:

$$f(t) = \left[\frac{log(\alpha)}{\alpha - 1}\right] \beta\omega v^{\gamma} \cdot (\omega v^{\gamma} t)^{(\beta-1)} \cdot e^{-(\omega v^{\gamma} t)^{\beta}} \cdot \alpha^{\left(1-e^{-(\omega v^{\gamma} t)^{\beta}}\right)} \quad (5)$$

Based on Equation (5) the CDF $(F(t))$, the survival $(S(t))$, and hazard $(h(t))$ are given by:

$$F(t) = \frac{\alpha^{\left(1-e^{-(\omega v^{\gamma} t)^{\beta}}\right)} - 1}{\alpha - 1} \quad (6)$$

$$S(t) = \frac{\alpha}{\alpha - 1}\left[1 - \alpha^{\left(-e^{-(\omega v^{\gamma} t)^{\beta}}\right)}\right] \quad (7)$$

$$h(t) = \frac{log(\alpha) \cdot \beta\omega v^{\gamma} \cdot (\omega v^{\gamma} t)^{\beta-1} \cdot e^{-(\omega v^{\gamma} t)^{\beta}} \cdot \alpha^{(1-e^{-(\omega v^{\gamma} t)^{\beta}})}}{1 - \alpha^{-e^{-(\omega v^{\gamma} t)^{\beta}}}} \tag{8}$$

The assumptions for the models presented from Equation (5) to Equation (8), establish that the parameters to be estimated $\alpha \neq 1$ and $\omega, v, \beta, \gamma > 0$. The voltage applied (v) to the ED must remain constant when obtaining the failure times through the ALT. In turn, given the flexibility that the IPL allows, Equation (5) to Equation (8) can also represent the reliability of ED if some other stress or variable is applied, such as current or load, which can be widespread variables for ED reliability analysis. On the other hand, the modeling presented in this section is not valid when it is intended to know the behavior of the ED under the effects of temperature since the IPL is not suitable for this modeling; for this case, the Arrhenius relation must be used.

In the following section, some statistical properties of APTW-IPL are shown in order to complement the reliability analysis.

4. Statistical properties of APTW-IPL

In this section, some statistical properties are described in order to be applied in the description of EDs under the effects of an ALT.

4.1. Quantile, median and mode

The $p-th$ quantile q_p of APTW-IPL, for $\alpha \neq 1$ can be obtained as:

$$q_p = \left\{ -\frac{1}{\omega v^{\gamma}} \cdot log\left[\frac{log(\alpha) - log(1 + p(\alpha - 1))}{log(\alpha)}\right]\right\}^{\frac{1}{\beta}} \tag{9}$$

The median can be obtained as:

$$q_{0.50} = -\frac{1}{\omega v^{\gamma}} \cdot log\left\{\frac{log(\frac{2\alpha}{\alpha+1})}{log(\alpha)}\right\}^{\frac{1}{\beta}}$$

The mode can be obtained by solving the following equation:

$$\frac{d}{dt}f(t) = 0 \rightarrow \frac{t^{\beta}}{\omega v^{\gamma}}\left(1 - log(\alpha)e^{-\left(\frac{t^{\beta}}{\omega v^{\gamma}}\right)}\right) - \beta + 1 = 0 \tag{10}$$

Equation Equation (10) can be solved numerically by iterative methods such as Newton-Raphson.

4.2. Moments

Let α^{-u} as a series representation expressed by:

$$\alpha^{-u} = \sum_{i=0}^{\infty}\left[\frac{\left(-log(\alpha)^{i} \cdot u^{i}\right)}{i!}\right] \tag{11}$$

Following Equation (11) the moment generation function (MGF) of the APTW-IPL described in (5) can be written as:

$$M_T(x) = \frac{\alpha}{1-\alpha}\sum_{i=0}^{\infty}\left[\frac{(-log\alpha)^{i+1}}{i!}\right] \cdot \sum_{i=0}^{\infty}\frac{x^j}{j!}\left[\frac{\Gamma\left(\frac{j}{\beta}+1\right)}{\left(\frac{1}{\omega v^{\gamma}}\right)^{\frac{j}{\beta}}(i+1)^{\frac{j}{\beta}+1}}\right] \quad (12)$$

Hence, the rth moment based on Equation (12) can be calculated as:

$$E(X^r) = \frac{\alpha}{1-\alpha}\sum_{i=0}^{\infty}\left[\frac{(-log\alpha)^{i+1}}{i!}\cdot\frac{\Gamma\left(\frac{r}{\beta}+1\right)}{\left(\frac{1}{\omega v^{\gamma}}\right)^{\frac{r}{\beta}}(i+1)^{\frac{r}{\beta}+1}}\right] \quad (13)$$

The characteristic function of APTW-IPL can be calculated as:

$$\phi_x(t) = \left(\frac{\alpha}{\alpha-1}\right) \cdot \sum_{i=0}^{\infty}\sum_{j=0}^{\infty}\left[\left(\frac{(i\lambda t)^j}{j!}\right)\left\{\frac{-log(\alpha)^{i+1}}{i!}\cdot\frac{\Gamma\left(\frac{r}{\beta}+1\right)}{\left(\frac{1}{\omega v^{\gamma}}\right)^{r/\beta}}(i+1)^{(r/b)+1}\right\}\right] \quad (14)$$

4.2.1. Conditional moments

For the APTW-IPL random variable, conditional moment is given as:

$$E(X^r|X>t) = \frac{1}{F(t)}\int_t^0 t^r f(t)dt$$

$$E(X^r|X>t) = \sum_{j=0}^{\infty}\frac{(log(\alpha))^{j+1}\left(1-\Gamma\left(\frac{r}{\beta}+1,\frac{t^{\beta}}{\omega v^{\gamma}}(1+j)\right)\right)}{j!(1+j)^{\frac{r}{\beta}+1}\left(\frac{1}{\omega v^{\gamma}}\right)^{\frac{r}{\beta}}\left(\alpha^{-e^{\left(\frac{t^{\beta}}{\omega v^{\gamma}}\right)}}-1\right)} \quad (15)$$

4.3. Mean residual life (MRL)

The MRL, is an important reliability metric to know the expected addtional lifetime after a reparation is made in the device, in this case the MRL can be estimated as:

$$\mu(t) = \frac{1}{S(t)}\left[E(t)-\int_0^t t\cdot f(t)dt\right]-t \quad (16)$$

For this case, $\int_0^t t\cdot f(t)dt$ based on the Equation (5) can be estimated as:

$$\int_0^t t \cdot f(t)dt = \frac{\alpha log(\alpha)}{\alpha - 1} \sum_{j=1}^{\infty} \left[\frac{-(log(\alpha))^j}{(j+1)! \cdot \left(\frac{j+1}{\omega v^\gamma}\right)^{\frac{1}{\beta}}} \right] \cdot \Gamma\left(\frac{(j+1)t^\beta}{\omega v^\gamma}; 1 + \frac{1}{\beta} \right) \tag{17}$$

Therefore, the MRL for the APTW-IPL can be written as:

$$\mu(t) = \frac{\Gamma\left(1+\frac{1}{\beta}\right)\left(\frac{1}{\omega v^\gamma}\right)^{-\frac{1}{\beta}} \sum_{j=0}^{\infty} \left[\frac{(-log(\alpha))^j}{j^{1/\beta} j!}\right] + log(\alpha) \sum_{j=0}^{\infty} \left[\frac{-log(\alpha))^j}{(j+1)!(\frac{j+1}{\omega v^\gamma})^{1/\beta}}\right] \Gamma\left[\frac{(j+1)t^\beta}{\omega v^\gamma}, 1+\frac{1}{\beta}\right]}{\alpha^{-e^{-(\omega v^\gamma t)^\beta}}} - t \tag{18}$$

4.4. Mean waiting time (MWT)

The MWT is the waiting time elapsed since a failure in the device had occured in the interval time $[0, t]$. The MWT can be calculated as:

$$\bar{\mu}(t) = t - \frac{1}{F(t)} \int_0^t t \cdot f(t)dt \tag{19}$$

Following the Equation (19) the MWT for the APTW-IPL is written as:

$$\bar{\mu}(t) = t - \frac{\alpha}{\alpha^{-e^{-(\omega v^\gamma t)^\beta}}} \cdot log(\alpha) \sum_{j=0}^{\infty} \frac{(-log(\alpha))^j}{(j+1)!\left(\frac{j+1}{\omega v^\gamma}\right)^{1/\beta}} \cdot \Gamma\left(\frac{(j+1)t^\beta}{\omega v^\gamma}, 1 + \frac{1}{\beta}\right) \tag{20}$$

4.5. Entropy

Given the nature of the life-stress model centered on EDs, it is important to calculate the entropy, which in this case will measure the uncertainty of the information obtained.

4.5.1. Shannon entropy

The Shannon Entropy can be defined as:

$$H_s = E[I(t)] = E[-log(f(t))] \tag{21}$$

By following Equation (21), the Shannon Entropy of Equation (5) is written as:

$$\begin{aligned} H_s &= 1 - \frac{\alpha \cdot log(\alpha)}{\alpha - 1} - log\left(\frac{\frac{\beta}{\omega v^\gamma} log(\alpha)}{\alpha - 1}\right) \\ &+ \frac{\alpha}{\alpha - 1} \sum_{j=0}^{\infty} \left[\frac{-log(\alpha)^{j+1}}{j!(j+1)} \cdot \left(\frac{1}{j+1} - \frac{\beta - 1}{\beta} \{\phi(1) - log(\beta) - log(j+1)\} \right) \right] \end{aligned} \tag{22}$$

4.5.2. Rényi entropy

The Rényi Entropy is defined as:

$$I_R(p) = \frac{1}{1-p} \cdot log \int_0^{\infty} f(t)^p dt \tag{23}$$

By following Equation (23), the Rényi Entropy of Equation (5) is written as:

$$\begin{aligned} I_R(p) \\ &= \frac{1}{1-p}\left[p \cdot log\left(\frac{\alpha log(\alpha)}{\alpha-1}\right)\right. \\ &+ (p-1) log\left(\frac{1}{\omega v^{\gamma}}\right) \\ &\left. - \frac{1-p}{\omega v^{\gamma}} \cdot log(\beta) + log\left(\sum_{i=0}^{\infty}\left\{\frac{(-log(\alpha p))^i \Gamma\left(p - \omega v^{\gamma} + \frac{\omega v^{\gamma}}{p}\right)}{i!(p+i)^{p\left(1-\omega v^{\gamma}+\frac{\omega v^{\gamma}}{p}\right)}}\right\}\right)\right] \end{aligned} \tag{24}$$

4.6. Order statistic

The k-out-of-n system structure is a very important and popular type of redundant system. Let $t_1, t_2 \ldots t_n$ a random sample from the APTW-IPL with PDF. Thus, the the PDF of the kth order statistic f_k is given by:

$$f_{k:n}(t) = n\binom{n-1}{k-1} F(t)^{k-1}(1-F(t))^{n-k} f(t) \tag{25}$$

By taking Equations (5) and (6) and replace them in Equation (25), the following is obtained:

$$\begin{aligned} f_{k:n}(t) &= \binom{n-1}{k-1} \beta\omega v^{\gamma}(\omega v^{\gamma} t)^{\beta-1} e^{-(\omega v^{\gamma} t)^{\beta}} \\ &\sum_{i=0}^{\infty}\sum_{j=0}^{\infty}(k-1)^i(n-k)^j\left(\frac{-1}{\alpha-1}\right)^i\left(\frac{\alpha}{\alpha-1}\right)^j \\ &\left[\alpha^{\left(1-e^{-(\omega v^{\gamma} t)^{\beta}}\right)}\right]^{i+1}\left[1-\alpha^{\left(-e^{-(\omega v^{\gamma} t)^{\beta}}\right)}\right]^j \end{aligned} \tag{26}$$

5. Time-varying APTW-IPL modeling

One of the aspects to consider within the reliability analysis for ED is the modeling of behavior when there is time-varying stress. For EDs, voltage variations on supply lines are an aspect that directly affects reliability and performance.

To establish the analysis in time-varying for ED, the IPL shown in Equation (4) can be modified as follows:

$$L = \left[\frac{\omega}{v(t)}\right]^{\gamma} \tag{27}$$

Where $v(t)$ It is a function that describes the voltage as a function of time and that this must be $v(t) > 0$ and $v(t)$ must be differentiable and integrable. Therefore, by taking Equation (26) and replace it in Equation (3), and considering the area under the curve that describes the time-varying stresss; the PDF of the APTW-IPL model is written as:

$$f(t,v(t))=\left[\frac{log(\alpha)}{\alpha-1}\right]\beta\left[\frac{v(t)}{\omega}\right]^{\gamma}\left\{\int_0^t\left[\frac{v(u)}{\omega}\right]^{\gamma}du\right\}^{\beta-1}\cdot$$
$$-\left\{\int_0^t\left[\frac{v(u)}{\omega}\right]^{\gamma}du\right\}^{\beta}\cdot\alpha\left(1-e^{-\left\{\int_0^t\left[\frac{v(u)}{\omega}\right]^{\gamma}du\right\}^{\beta}}\right) \tag{28}$$

The equations of $F(t,v(t)), R(t,v(t))$ and $H(t,v(t))$ can be derived from Equation (28) and following the classical formulation for the essential reliability functions.

6. MLE of APTW-IPL

Let $v_i, i=1,2,\ldots\theta$, the voltage applied in the piece under the ALT and $t_{i,j}=1,2,\ldots,\rho,$ the failure time of the piece induced by the voltage stress level v_i; thus, by taking the log function of Equation (5), the log-likelihood can be written as:

$$\begin{aligned}\ell &= \theta\rho\cdot log\left[\frac{log(\alpha)}{\alpha-1}\right]\\ &+\theta\rho\cdot log(\beta)+\theta\rho\cdot log(\omega)+\gamma\cdot\sum_{i=1}^{\theta}[log(v_i)]\\ &+(\beta-1)\cdot\sum_{i=1}^{\theta}\sum_{j=1}^{\rho}\left[log\left(\omega v_i^{\gamma}t_{i,j}\right)\right]\\ &-\sum_{i=1}^{\theta}\sum_{j=1}^{\rho}\left[\left(\omega v_i^{\gamma}t_{i,j}\right)^{\beta}\right]\\ &+log(\alpha)\cdot\sum_{i=1}^{\theta}\sum_{j=1}^{\rho}\left[1-e^{-\left(\omega v_i^{\gamma}t_{i,j}\right)^{\beta}}\right]\end{aligned} \tag{29}$$

By taking the first partial derivative of Equation (29), the estimation for each parameter $\alpha, \beta, \omega,$ and γ can be calculated as follow:

$$\frac{\partial\ell}{\partial\alpha}=\frac{\theta\rho}{\alpha\cdot log(\alpha)}-\frac{\theta\rho}{\alpha-1}+\frac{1}{\alpha}\cdot\sum_{i=1}^{\theta}\sum_{j=1}^{\rho}\left[1-e^{-\left(\omega v_i^{\gamma}t_{i,j}\right)^{\beta}}\right] \tag{30}$$

$$\begin{aligned}\frac{\partial\ell}{\partial\beta} &= \sum_{i=1}^{\theta}\sum_{j=1}^{\rho}\left[\left(\omega v_i^{\gamma}t_{i,j}\right)^{\beta}\right.\\ &\left.\cdot log\left(\omega v_i^{\gamma}t_{i,j}\right)\cdot\left\{log(\alpha)\cdot e^{-\left(\omega v_i^{\gamma}t_{i,j}\right)^{\beta}}-1\right\}+log\left(\omega v_i^{\gamma}t_{i,j}\right)\right]\end{aligned} \tag{31}$$

$$\frac{\partial \ell}{\partial \omega} = \frac{\theta\beta\rho}{\omega} + \frac{\beta}{\omega} \cdot \sum_{i=1}^{\theta}\sum_{j=1}^{\rho}\left[\left(\omega v_i^{\gamma} t_{i,j}\right)^{\beta} \cdot \left\{log(\alpha) \cdot e^{-\left(\omega v_i^{\gamma} t_{i,j}\right)^{\beta}} - 1\right\}\right] \tag{32}$$

$$\frac{\partial \ell}{\partial \gamma} = \beta\sum_{i=1}^{\theta}[log(v_i)] + \beta\sum_{i=1}^{\theta}\sum_{j=1}^{\rho}\left[log(v_i) \cdot \left(\omega v_i^{\gamma} t_{i,j}\right)^{\beta} \cdot \left\{log(\alpha) \cdot e^{-\left(\omega v_i^{\gamma} t_{i,j}\right)^{\beta}} - 1\right\}\right] \tag{33}$$

The Fisher information matrix based on Equation (30) to Equation (33) is given by:

$$J(\delta) = -\begin{bmatrix} I_{\alpha\alpha} & I_{\alpha\beta} & I_{\alpha\omega} & I_{\alpha\gamma} \\ I_{\beta\alpha} & I_{\beta\beta} & I_{\beta\omega} & I_{\beta\gamma} \\ I_{\omega\alpha} & I_{\omega\beta} & I_{\omega\omega} & I_{\omega\gamma} \\ I_{\gamma\alpha} & I_{\gamma\beta} & I_{\gamma\omega} & I_{\gamma\gamma} \end{bmatrix} \tag{34}$$

where the elements of the matrix are defined in Appendix A, the computation of Equation (34) were made in R via MaxLik Package (Henningsen & Toomet, 2011).

To obtain the confidence interval we based on the asymptotic normality of MLE's. The $100(1-\zeta)\%$ confidence intervals for $\alpha, \beta, \omega, and \gamma$ are given by:

$$\left(\hat{\alpha} \pm z_{1-\rho/2}\sqrt{var(\hat{\alpha})}\right) \tag{35}$$

$$\left(\hat{\beta} \pm z_{1-\rho/2}\sqrt{var\left(\hat{\beta}\right)}\right) \tag{36}$$

$$\left(\hat{\omega} \pm z_{1-\rho/2}\sqrt{var(\hat{\omega})}\right) \tag{37}$$

$$\left(\hat{\gamma} \pm z_{1-\rho/2}\sqrt{var(\hat{\gamma})}\right) \tag{38}$$

where $z_{1-\rho/2}$ is the upper $(\rho/2)$ percentile of the standard normal distribution.

7. Case studies

In this section, the life–stress relationship presented in Equation (5) is implemented in two case studies based on ED. The first case study is based on determining the performance and reliability of a micro-motor (DCMM). The DCMM is a fundamental part of the system that allows the extraction and release of the sheet of a cassette containing a medical study. The medical device is based on digitizing images through Computerized Radiology (CR) taken through an X-ray system. CRs have become a new generation tool in the medical diagnostics sector.

The second case study is based on a Linear Variable Differential Transformer (LVDT). An LVDT is a type of electrical transformer used for measuring linear displacement (position) in the industry. This device bases its operation on the movement of a core inside the sensor's body with the windings wound; hence it is essentially a transformer with its moving core. The LVDT analyzed

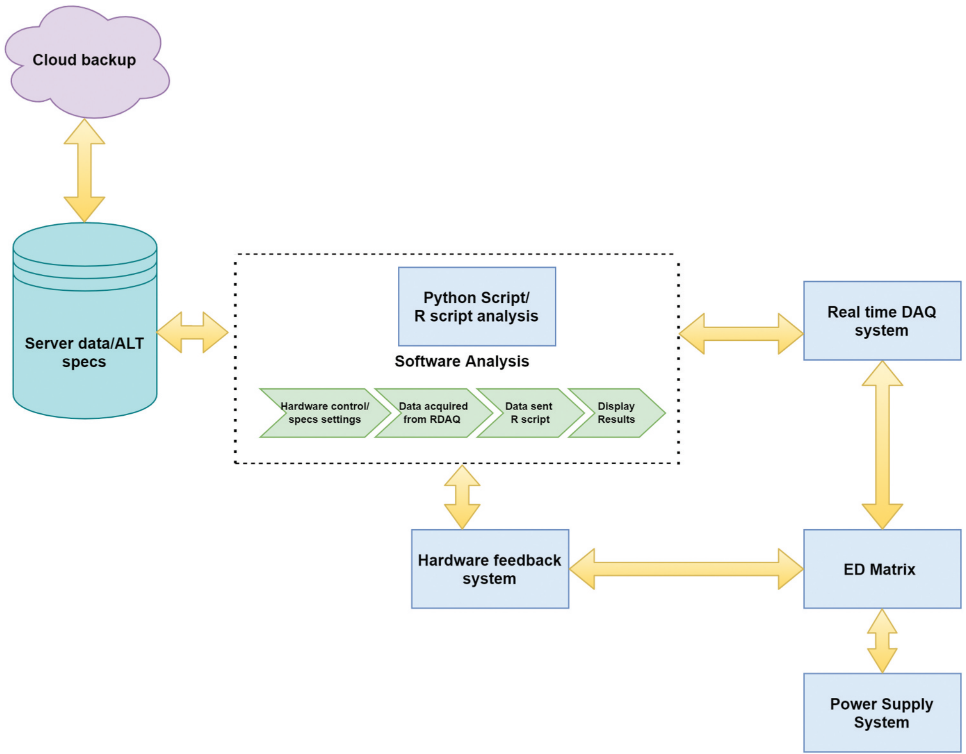

Figure 3. PDF for some parameter values derived of APTW.

in this case study is located in test equipment that verifies the presence and depth at which a series of screws are located in an upper casing used in turbos of engines in the automotive sector. If there is an absence of these screws, liquid such as water can leak directly into the gear system causing general failure in the engine turbo system.

The failure time of the devices under analysis was obtained via ALT, where the applied stressor variable was voltage (v) set in DC volts. The conditions and test plan of each device are described in the corresponding section. An automated ALT was programmed via Python 3.8 script, a Real-Time Data Acquisition system, and an R script for data collection. Figure 3 shows the schematic diagram of information acquisition and data processing.

Table 1. Summary of pdf's of other bathtub models under IPL.

Model	PDF
BGWD	$f(t)=\frac{ac\left(\frac{1}{\omega v^{\gamma}}\right)^{c}\cdot t^{c-1}}{B(a,\beta)}\left(1-e^{-\left(\frac{t}{\omega v^{\gamma}}\right)^{c}}\right)^{aa-1}\left[1-\left(1-e^{-\left(\frac{t}{\omega v^{\gamma}}\right)^{c}}\right)^{a}\right]^{\beta-1}e^{-\left(\frac{t}{\omega v^{\gamma}}\right)^{c}}$
BW	$f(t)=\frac{\Gamma(a+\beta)}{\Gamma(a)\Gamma(\beta)}c\omega v^{\gamma}(\omega v^{\gamma}t)\left[1-e^{-(\omega v^{\gamma}t)^{c}}\right]^{a-1}e^{-\beta(\omega v^{\gamma}t)^{c}}$
GED	$f(t)=\frac{a}{\omega v^{\gamma}}\left[1-e^{-\left(\frac{t}{\omega v^{\gamma}}\right)}\right]^{a-1}e^{-\left(\frac{t}{\omega v^{\gamma}}\right)}$
EXW	$f(t)=\omega v^{\gamma}a\beta(\omega v^{\gamma}t)^{a-1}\left[1-e^{-(\omega v^{\gamma}t)^{a}}\right]^{\beta-1}e^{-(\omega v^{\gamma}t)^{a}}$
AWD	$f(t)=\frac{1}{\omega v^{\gamma}}\cdot\left(at^{a-1}-\beta t^{\beta-1}\right)\cdot e^{-\frac{t^{a}-t^{\beta}}{\omega v^{\gamma}}}$

On the other hand, to test the effectiveness of the life-stress model, a comparative study with other methodologies that describe the behavior of the bathtub curve of the failure times is presented, such as, the AWD, BW, EXW models, the list of models compared is presented in Table 1. Finally, in both case studies, the parameters' estimation was programmed in R using the maxLik package (Henningsen & Toomet, 2011).

7.1. Case of study 1. Reliability study of DCMM

For this case of study, a DCMM is under analysis. The assumptions of the ALT performed to de DCMM are the following:

• Three test levels were established at $15v$, $18v$, and $21v$. The voltage levels were set on constant stress.

• No censored data were considered for this ALT.

• The level of use condition for this case is at $3.3v$ at $1A$.

• All failure times were obtained when the DCMM was without a load.

The results of the ALT can be seen in Table 2.

Table 2. ALT failure time of DCMM under voltage stress.

Stress	$15v$	$18v$	$21v$
Time (in Hours)	366	217	140
	5226	3108	2002
	6181	3676	2368
	3812	2267	1461
	5506	3274	2110
	572	340	219
	537	319	205
	4621	108	1767
	181	347	69
	583	2742	223
	7110	4228	2725
	4846	2882	1857

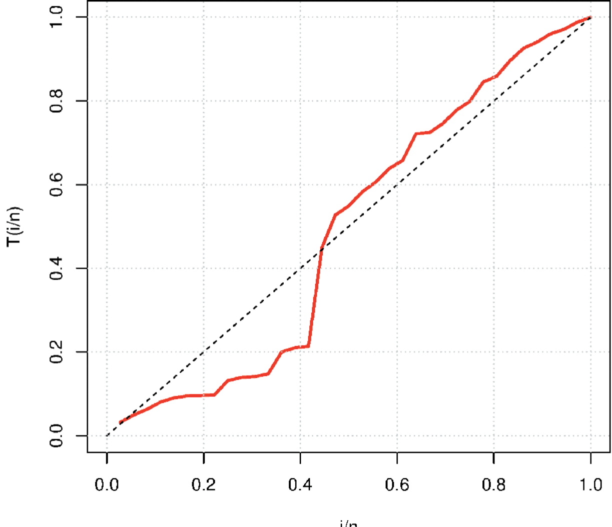

Figure 4. TTT plot for the data obtained in Table 2.

In the first instance, it is necessary to verify if the data obtained in Table 2 is candidate to have a bathtub curve behavior, so in Figure 4, the TTT plot is shown. The TTT plot was programmed in R using the Adequacy Model package Diniz Marinho et al. (2016).

The visual performance presented in Figure 4 shows that the data in Table 2 is candidate to have a behavior in its failure rate in the form of a bathtub curve, this taking into account the established by Aarset (1987). Therefore, taking the values of Table 2 and substituting them in the MLE functions from Equation (30) to Equation (33) and the corresponding MLE equations of the models presented in Table 1, the values of the parameters of each model can be estimated. The results of the parameter estimates are shown in Table 3.

From the results obtained in Table 3, it is possible to plot the DCMM's performance under voltage stress and the different bathtub shape distributions. Figure 5 shows the PDF behavior of the DCMM at voltage use condition $(3.3v)$. In the first instance, the PDF presented in Figure 5, we can notice the different behaviors that DCMM has when analyzed by the models presented in Table 1. Another aspect to highlight in the PDF presented in Figure 5 is how the parameter α of the APTW-IPL model affects the shape; the PDF of the DCMM under the APTW-IPL is biased on the right in comparison to the other models under analysis. This bias modifies the probability region of the lifetimes of the DCMM in operation, allowing them to be in a slightly broader region concerning the other life-stress models and modifying the highest point of the PDF. This modification causes quality aspects such as warranty and maintenance times to be substantially modified. Therefore, it highlights the importance of making a correct choice of the model that describes the device more closely to its normal usage with the customers.

In Figure 6, the behavior of the reliability plot of the DCMM under the different bathtub shape models is shown; the Figure 6 was plotted at DCMM nominal voltage $(3.3v)$. In this case, the proposed APTW-IPL model shows that its curve behavior is more closed than the models under analysis. This behavior is due to the value of the parameter γ for each of the models under analysis. In the reliability field, the parameter γ measures the effect of the stress applied (in this case, the voltage) on the device's useful life. Therefore, if the value of γ is high, the life of the device is shortened operationally, which can directly affect the estimation of the warranty times that can be offered. To demonstrate these differences, Table 4 shows the MTTF calculations for each of the models presented in Table 1. The MTTF was calculated at the DCMM nominal voltage operation.

The MTTFs presented in Table 4 showed that the device under the APTW-IPL estimates $4,509$ hours less than the GED-IPL model, $7,887$ hours less than BW-IPL model, 9636 hours less than AWD-IPL model, $11,523$ hours less than BGWD-IPL, and $14,482$ hours less than EXW-IPL model.

Figure 7 shows the behavior of the DCMM failure rate when the nominal voltage $(3.3v)$ is applied to the device. Observing the behavior of the DCMM under the models BGWD-IPL, BW-IPL, GED-IPL, EXW-IPL, and AWD-IPL, it is appreciated that the failure rate of the DCMM exhibits a behavior with a tendency of a " V "or a shortened "J". Having as evidence that the data adjust towards a non-monotonic behavior but a good fit to represent the bathtub curve in a good way, they conform to a bathtub curve behavior, which indicates that the APTW-IPL model can more adequately describe the use of ED in real operational environments.

To demonstrate if the APTW-IPL model could be the best choice to describe the device's behavior under analysis. A goodness-of-fit test is presented in Table 5, where the Akaike Information Criteria (AIC), Bayesian Information Criteria (BIC), Kolmogorov-Smirnov (KS), Cramér-von-Mises (W) and Anderson-darling (A), and P-value is presented.

The results obtained in Table 5 show that the APTW-IPL could be chosen as the best model among the fitted models since it has the lowest values of the AIC and BIC. The fitting can be demonstrated graphically using the Probability-Probability (PP) plots for the data presented in Table 2, therefore in Figure 8 the results obtained from the PP plots adjustments are shown.

Table 3. Estimated values and their standard errors in brackets for the data provided in Table 2.

Model	α	β	ω	γ	a	c
APTW-IPL	10.5782(0.01478)	0.9547(0.0451)	$1.7894e-06(1.0247e-03)$	2.7147(0.1478)	–	–
BGWD-IPL	19.2891(0.3784)	0.9747(0.0677)	$2.2344e-06(3.5591e-03)$	2.3714(0.2259)	$0.5582(1.447e-03)$	2.9097(0.3347)
BW-IPL	22.7819(0.5579)	0.55748(0.0447)	$9.1014e-06(2.2547e-04)$	2.4149(0.3547)	–	2.2478(0.4271)
GED-IPL	12.2593(0.7789)	–	$1.1478e-05(3.6657e-03)$	2.5478(0.1147)	–	–
EXW-IPL	4.9954(0.6578)	0.9948(0.1147)	$3.5760e-07(3.336e-04)$	2.2145(0.2598)	–	–
AWD-IPL	2.4898(0.1489)	5.0784(0.3547)	$4.5979e-08(4.7781e-03)$	2.4389(0.3353)	–	–

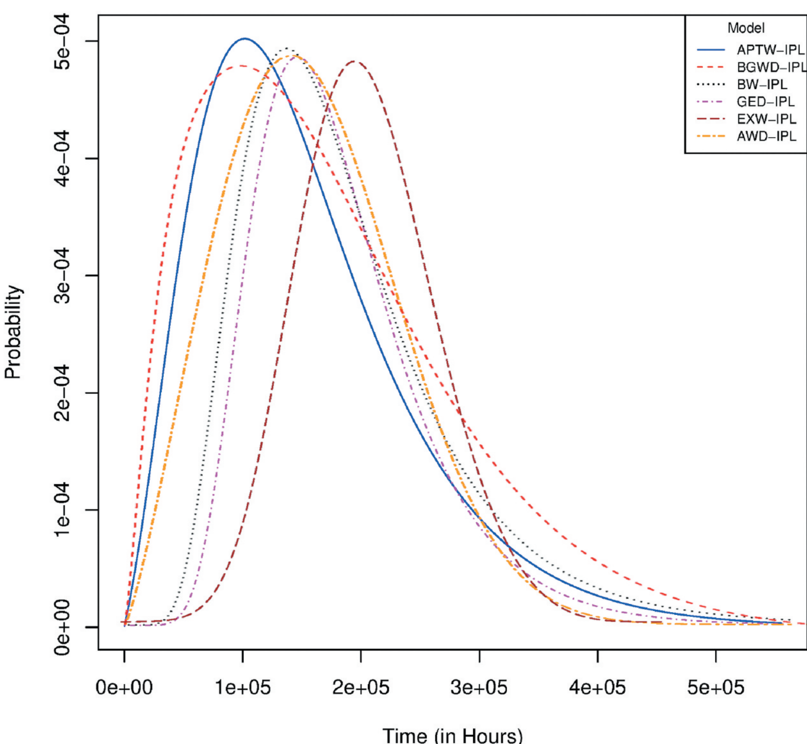

Figure 5. PDF of the DDCM under bathtub shape models at nominal voltage operation $(3.3v)$.

7.1.1. Discussion of results and physical meaning of APTW-IPL in the DCMM

Based on the results obtained for the DCMM, it can be established that the APTW-IPL model offers a better description of the device that includes the estimation of failure times, the description of the failure rate in the form of a bathtub, and the adjustment of data from an ALT. With this information, it is possible to increase and improve the quality of the product. However, to achieve these improvements, it is necessary to know the meaning of each parameter within the device under analysis.

An important aspect to highlight is the difference in the methodologies. The failure rates represent the MTTF's differences, which is used as a metric measure to identify the average time of the device before some maintenance or repair. As shown in Table 4, the differences of the MTTF are very marked for each model under the analysis. In this case, reliability engineers can choose the APTW-IPL model as the most viable option based on two premises. The first one in which the APTW-IPL model estimates fewer MTTF times for the DCMM, which may result in a model with a higher MTFF, a flawed calculation of the maintenance and warranty times of the device may be incurred. On the other hand, the adjustment of the ALT data should be considered part of the initial selection for the analysis of the device. As shown in Table 5, the APTW-IPL has an advantage over the GED-IPL by considering the P-value produced by both models.

Another aspect to consider is the description of the parameters of the APTW-IPL model in the DCMM. The parameter ω measures the losses generated in the device's internal components under analysis. For the DCMM, parameter ω is reflected in the brushes, the motor coil, and the magnet, which are affected by the increase in temperature and current when subjecting them to voltage overstress. On the other hand, the parameter ω establishes a relation of the maximum efficiency that the motor can offer under a normal operating voltage and the current. As can be seen in the APTW-

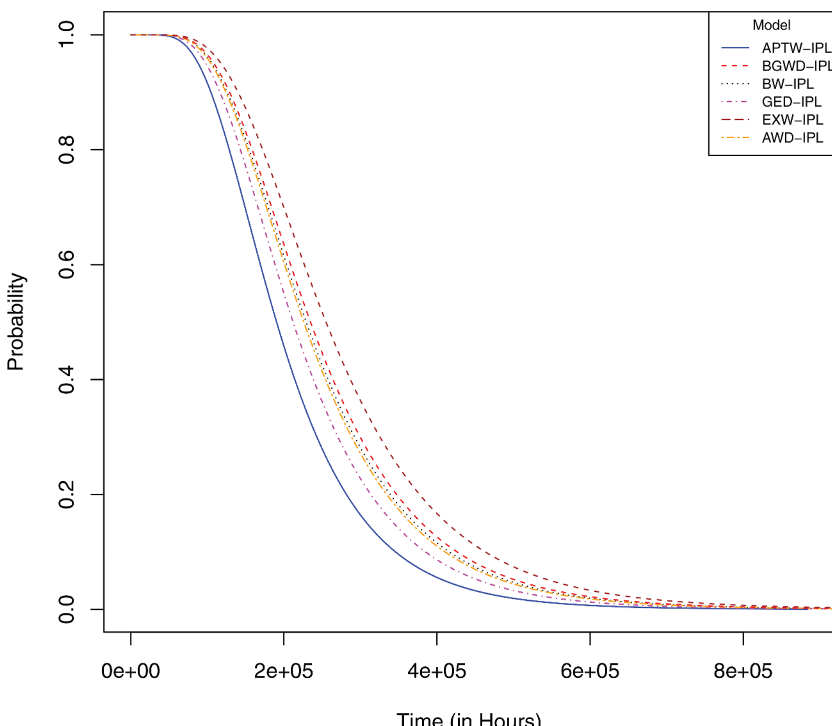

Figure 6. Reliability plot of the DDCM under bathtub shape models at nominal voltage operation $(3.3v)$.

Table 4. MTTF values of DCMM in nominal voltage operation $(3.3v)$ and the values obtained in Table 3.

Model	MTTF (In Hours)
APTW-IPL	230, 478
BGWD-IPL	242, 001
BW-IPL	238, 365
GED-IPL	234, 987
EXW-IPL	244, 960
AWD-IPL	240, 114

IPL model, the minimal efficiency ratio is compared to the other models in which the DCMM is compared. Finally, practically, the parameter ω is associated with the quality of the materials with which the device is manufactured.

The parameter γ establishes how the life of the device is affected by the voltage applied during ALT. A high value of the parameter γ establishes that the life is reduced more quickly as the device is being used. This statement can be supported with the information shown in Table 4, where the APTW-IPL model shows that the life of the DCMM is less than if it is expressed under other models with the shape of a bathtub. In a practical way, the parameter γ is associated with the resistance of the materials; in the case of the DCMM, it would be the reduction of the resistance between the terminals that energize the motor, the brushes, and the coil.

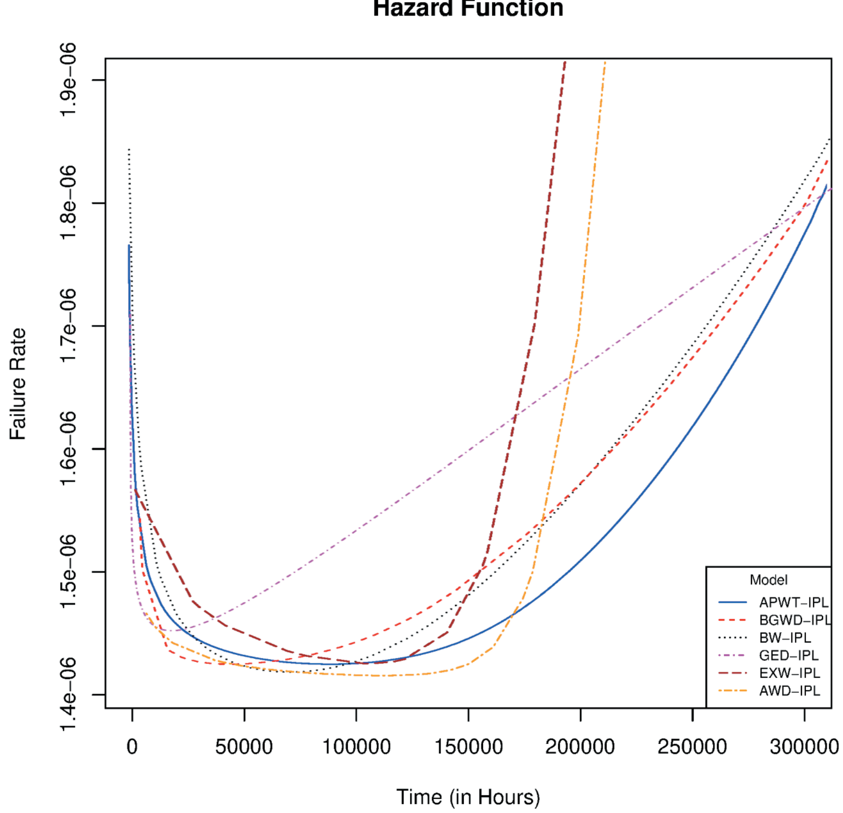

Figure 7. Failure rate of the DCMM under bathtub shape models at nominal voltage operation $(3.3v)$.

Table 5. Summary values of the models fitted to the DCMM.

Model	AIC	BIC	KS	W	A	P-Value
APTW-IPL	206.4451	209.3214	0.1065	0.1314	0.2014	0.9017
BGWD-IPL	225.3647	223.4782	0.2514	0.2767	0.3547	0.7314
BW-IPL	213.7789	216.3657	0.1647	0.1836	0.2647	0.8136
GED-IPL	209.7891	212.3354	0.1433	0.1512	0.2347	0.8560
EXW-IPL	229.1472	227.3577	0.2714	0.2914	0.3965	0.6914
AWD-IPL	217.9871	220.3312	0.2014	0.2165	0.3047	0.7914

Parameters α and β represent a shape parameter and marked effects on the behavior of the lifetime and failure time distribution of DCMM. Moreover, differences in those parameters affect the estimation of the lifetime and performance of the DCMM directly, as can be seen in the calculation of the MTTF presented in Table 4.

The above presented were reflected in the DCMM failures, which we can list the following: During Infant Mortality exhibited in Figure 7 the associated failures of DCMM are:

- **Failure in the bearings** which causes a bad installation, there is excessive consumption of nominal power in the DCMM causing early Failure.
- **Bad assembly of the moving elements of the DCMM**, which will cause an incorrect tensioning of the belt and premature wear of it, abnormal power consumption, and noise.
- At the useful stage exhibited in Figure 7 the associated failures of DCMM are:

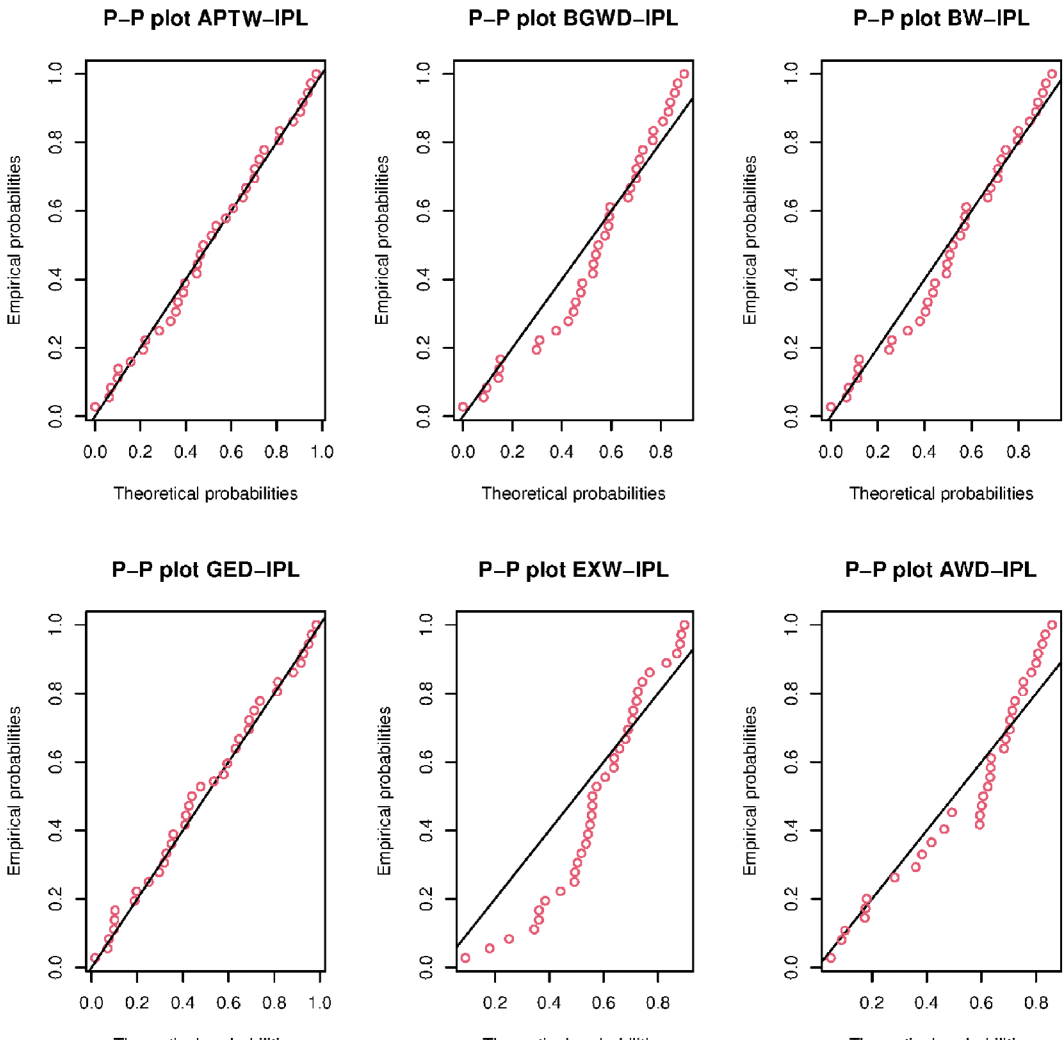

Figure 8. P-P plots for DCMM.

- **Resistance in the motor armature**, which allows the passage of current. So, when the resistance decreases, the temperature inside the device increases, accelerating the wear of the motor terminals and causing the fault. For this experiment, the armature resistance registered an average decrease of 7% from the nominal value.
- Finally, at the wear-out stage exhibited in Figure 7 the associated failures of DCMM are:
- **Motor shaft** is the one that has the most significant impact on the wear stage; this is due to the stresses generated in the environment and the load that the DCMM moves during its useful life.
- **Motor brushes** in this case, it is presented by the loss of armature resistance which induces a more significant current. Given the nature with which the brushes are manufactured, they suffer exponentially increasing wear.

7.2. Case of study 2. reliability study of LVDT

To determine the behavior of the LVDT under voltage stress, an ALT was performed, which follows the following assumptions:

- Three test levels were established at $18v$, $21v$, and $23v$. The voltage levels were set on constant stress.
- No censored data were considered for this ALT.
- The level of use condition for this case is at $5v$ at $500mA$.

The results of the ALT can be seen in Table 6.

Following the same procedure as in Case of Study 7.1, the data obtained in Table 6 is checked if these are candidates to have a bathtub curve behavior, the result of the TTT plot is shown in Figure 9.

If we are reviewing the performance of Figure 9, it is concluded that the LVDT data presented in Table 6 present a bathtub curve behavior. Therefore, we proceed to estimate the parameters of the APTW-IPL model, so Table 7 shows the results of these estimates.

Based on the results obtained in Table 7, the PDF that describes the behavior of the LVDT under the nominal voltage at $5v$ is presented in Figure 10.

As shown in Figure 10, the behavior of the LVDT probability under the APTW-IPL, GED-IPL, and AWD-IPL models does not offer a closed area compared to the other models analyzed. This PDF behavior is due to the slight variations presented by the LVDT when subjected to ALT. Since the data handled by the LVDT must be processed in A/D conversion by a transducer, there may be slight truncations of information that the models mentioned above can not fully grasp. Nevertheless, these slight variations do not significantly affect the calculation of the device's behavior under analysis.

In Figure 11, it can see the reliability of the LVDT under the nominal voltage level. This graph gives us the information that the LVDT under the APTW-IPL model exhibits a lower MTTF, which indicates that the device has a shorter lifetime, so the warranty information provided by the manufacturer can be affected if the device is not modeled under the proper probability distribution. Given this premise, Table 8 shows the MTTF values for each of the models analyzed for the LVDT.

The results of the MTTF for the LVDT under the different methodologies showed different calculations. It can be seen that under the APTW-IPL modeling, the LVDT estimates 6,179 less than under the AWD-IPL model, 8,136 hours less than the EXW-IPL model, 11,634 hours less than the BW-IPL model, 14,723 hours less under the BGWD-IPL model, and 17,636 hours less under the GED-IPL model.

The failure rate of the LVDT under nominal voltage is presented in Figure 12

The behavior of the LVDT failure rate under the APTW-IPL model resembles a bathtub curve. However, this curve turns out to have a steeper curve on the left side, which establishes an indication that the infant mortality of the device is prolonged a little more than what the theory of devices with bathtub curve behavior establishes. On the other hand, under the models established in Table 1, the LVDT failure rate shows a behavior similar to a J or an elongated U. The J or U-shaped behavior can be taken as a bathtub shape. However, the adjustment of the LVDT failure times under the APTW-IPL model is much better. Table 9 shows the AIC, BIC, A, W, and KS values for the LVDT data and the bathtub shape models.

Table 6. ALT failure time of LVDT under voltage stress.

Stress	$18v$	$21v$	$23v$
	128	76	55
	135	80	59
	153	91	67
	525	312	229
	1296	770	566
Time	2093	1244	915
(in Hours)	2115	1257	924
	2604	1548	1139
	3274	1946	1431
	3434	2041	1501
	3567	2120	1559
	3749	2228	1639

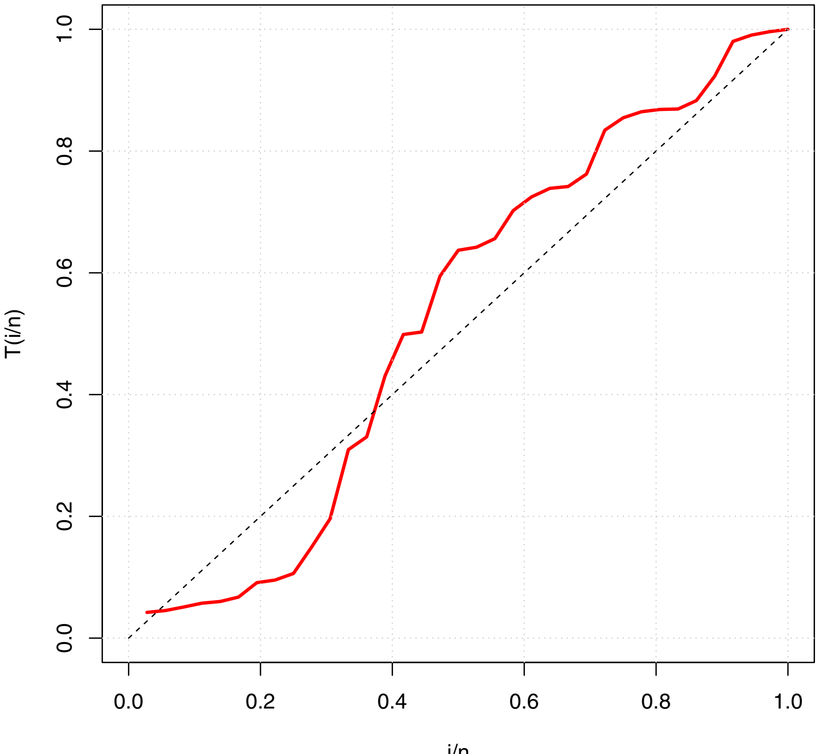

Figure 9. TTT plots for the LVDT data presented in.Table 6

P-P plots of the distributions for data sets in Table 6 is presented in Figure 13.

7.2.1. Discussion of results and physical meaning of APTW-IPL in the LVDT

In this case study, we can also highlight the difference of the MTTF between the models studied. This difference is due to the value of the parameter γ estimated in Table 7. It can be observed that the LVDT under the APTW-IPL model has a higher value than the other models under analysis. The useful life of the device is significantly reduced. In turn, as shown in Figure 13, the fit of the LVDT data presented in Table 6 has better compatibility with the APTW-IPL model concerning the other models put under analysis. In this case, for practitioners, the APTW-IPL model may be the best option as a descriptor of failure times for the LVDT. The physical interpretation of the parameters of the APTW-IPL model on the LVDT are very similar to those established in section 7.1.1, so by centering it on the LVDT, we can establish the following.

The parameter ω that measures the internal losses in the device under analysis shows that in the case of the LVDT, the elements that will suffer the most damage are: the Analog-Digital converter, the coils that surround the core of the LVDT, the secondary windings, Electromagnetic Shielding, and the resistance from the LVDT signal conductor to the processing module.

As stated above, the parameter γ is reflected in the life of the device. For the LVDT, the voltage effects can be measured by the MTTF calculated when the device is supplied with the nominal voltage.

Parameters α and β represented a shape parameter and marked effects on the behavior of the lifetime and failure time distribution of LVDT. The effects of these parameters can be seen in the Figures from 10 to Figure 12.

The above presented were reflected in the LVDT failures, which we can list the following:

During Infant Mortality exhibited in Figure 12 the associated failures of DCMM is:

Table 7. Estimated values and their standard errors in brackets for the LVDT data provided in Table 6.

Model	α	β	ω	γ	a	c
APTW-IPL	15.7891(0.1369)	0.9817(0.0578)	$9.6781e-08(1.4521e-02)$	3.5793(0.2245)	–	–
BGWD-IPL	21.9784(0.3657)	0.9293(0.0657)	$1.1234e-10(6.4789e-02)$	2.8987(0.3014)	0.9582(0.0147)	3.9790(0.2978)
BW-IPL	18.9732(0.1478)	0.8914(0.0101)	$9.4789e-09(3.3241e-03)$	2.9930(0.4547)	–	3.6578(0.5478)
GED-IPL	1.2593(0.4781)	–	$8.1478e-09(2.5971e-03)$	2.6890(0.3524)	–	–
EXW-IPL	2.0224(0.2987)	0.9023(0.2047)	$6.6242e-08(3.9871e-04)$	3.1981(0.3596)	–	–
AWD-IPL	5.4898(0.2499)	6.0784(0.1547)	$4.5979e-08(4.7781e-03)$	3.3765(0.2547)	–	–

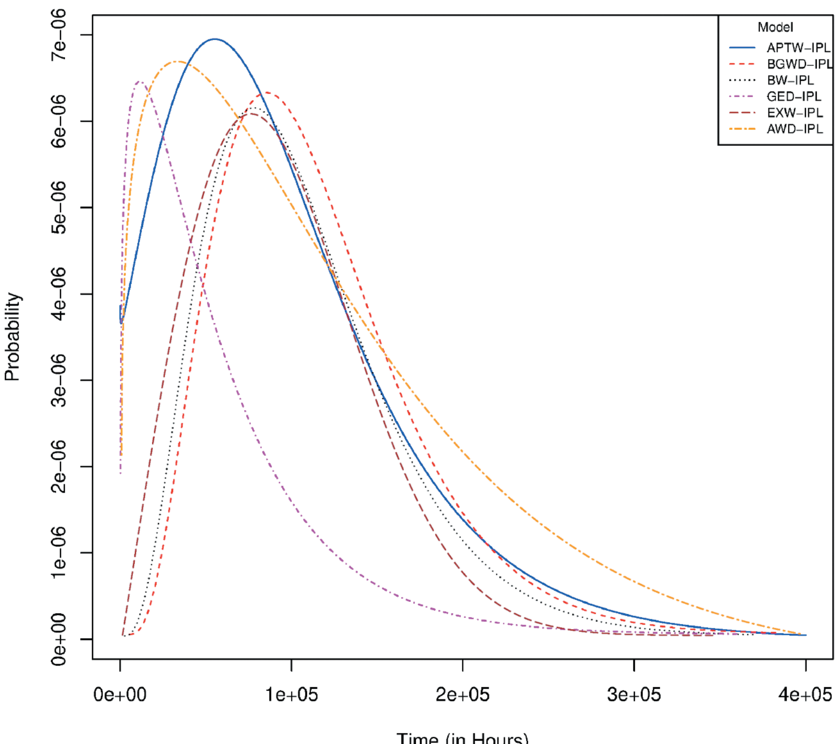

Figure 10. PDF plot for LVDT under bathtub shape models at nominal voltage operation.

- **Electromagnetic Shielding** This early fault causes a decompression in the current circulating through the LVDT windings, inducing an efficiency leakage, thus at the moment of sending the data to the analog-digital converter.
- At the useful stage exhibited in Figure 12 the associated failures of LVDT are:
- **Internal resistance of LVDT main and secondary windings**, which allows the passage of current. For this fault, there are two problems; the first is the increase in temperature due to the excess current between the windings, causing wear in the protection of the copper cable. The second associated failure is towards the data sent to the LVDT conversion towards the analog-digital converted device.
- Finally, at the wear-out stage exhibited in Figure 7 the associated failures of DCMM are:
- **LVDT wiring** The faults presented in this part of the LVDT cause that the measurements are not adequate, having to adjust the gain of the converter continuously.
- **Analog-Digital Module**, since this module is in charge of processing the information of the LVDT, in this case, due to current variations, wear in the protection of the winding cables, and excess temperature in the conductors, the converter module is affected, causing failures associated with wear by essential LVDT components

8. Conclusion and future scope

This article presented a model based on the APT combined with the WD and the IPL. The purpose of this life–stress relationship was to establish a better fit to the data from an ALT to describe the behavior of ED, which, due to its complex systems based on semiconductors, shows a bathtub behavior in their failure rate.

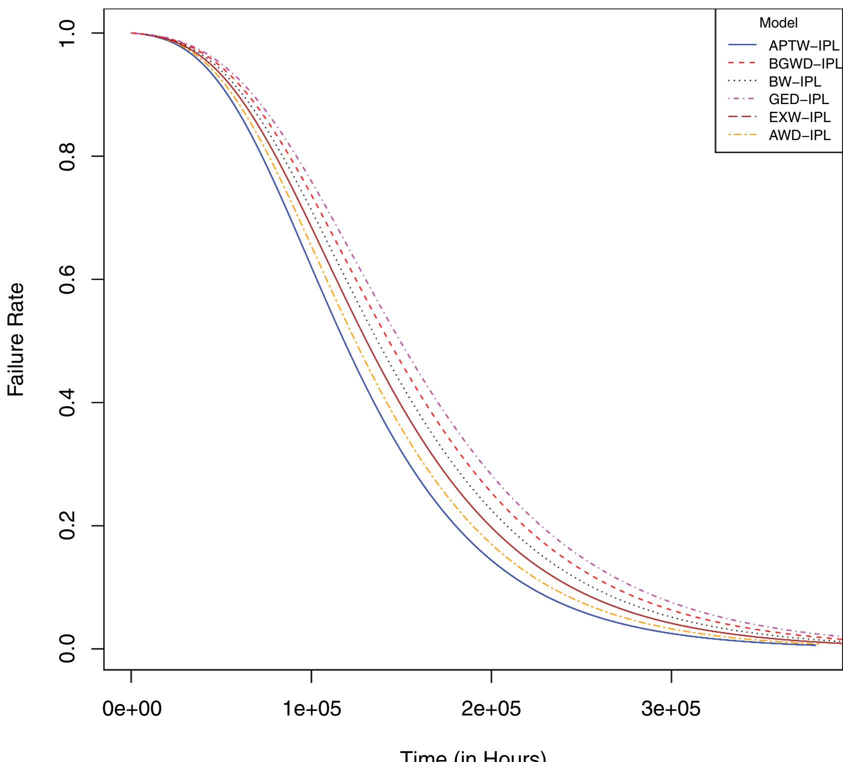

Figure 11. Reliability plot for LVDT under bathtub shape models at nominal voltage operation.

Table 8. MTTF value obtained for the LVDT at nominal voltage $(5v)$.

Model	MTTF (In Hours)
APTW-IPL	123, 478
BGWD-IPL	138, 201
BW-IPL	135, 112
GED-IPL	141, 114
EXW-IPL	132, 014
AWD-IPL	129, 657

The APTW-IPL was tested in two scenarios based on DCMM and LVDT. In both cases, the bathtub failure rate was checked via a TTT plot. A comparative study was carried out with five other methodologies based on the description of the failure rates in a bathtub curve: the GBWD-IPL, BW-IPL, GED-IPL, EXP-IPL, and AWD IPL. The parameters, reliability graphs, the MTTF and P-P plots were obtained for both case studies to understand each model under analysis and establish a discussion. The presented evidence throughout the article showed that the APTW-IPL model might be the best option to describe an ED's behavior under a level of voltage stress; this is based on the failure rate shape and the evidence provided in Tables 5 and 9. Additionally, a physical description of the APTW-IPL parameters was established; in order that the reliability engineers can improve the quality and MTTF of the EDs.

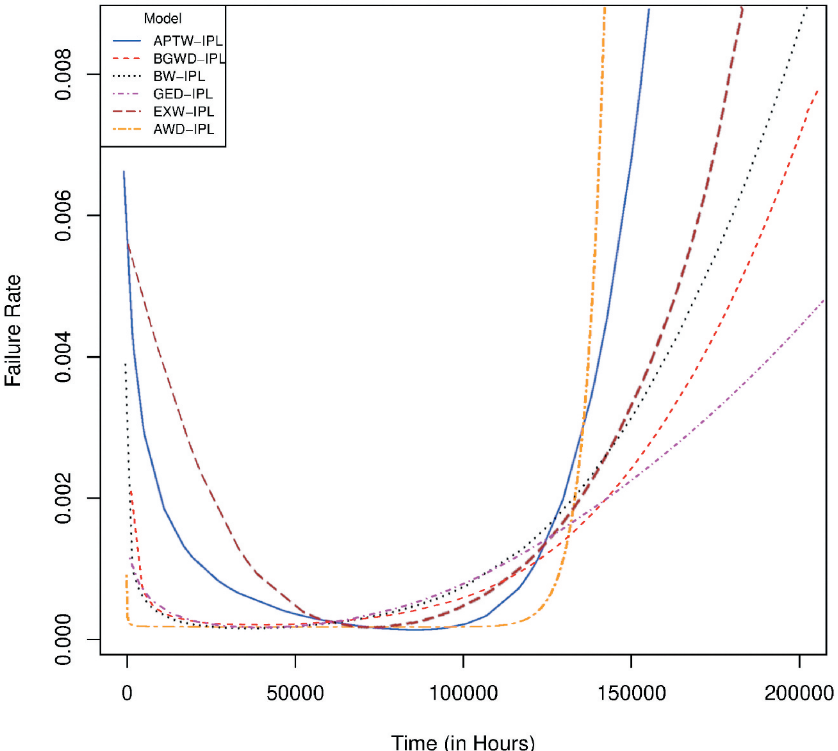

Figure 12. Failure rate plot for LVDT under bathtub shape models at nominal voltage operation $5v$.

Table 9. Summary values of the models fitted to the LVDT.

Model	AIC	BIC	KS	W	A	P-Value
APTW-IPL	250.1147	252.3014	0.1145	0.1488	0.1874	0.9120
BGWD-IPL	263.9324	265.6567	0.2587	0.2767	0.3214	0.7877
BW-IPL	259.8932	262.1467	0.2044	0.2241	0.2799	0.8036
GED-IPL	263.1798	270.3478	0.3147	0.3398	0.3677	0.6514
EXW-IPL	256.2571	259.9855	0.1719	0.1944	0.2442	0.8454
AWD-IPL	253.9871	255.3312	0.1414	0.1644	0.2114	0.8825

A future work proposed for this model is to analyze the effects of the time-varying voltage such as electrical harmonics situation by substituting $v(t)$ presented in Equation (28) for the Fourier series that describes the voltage stress at that moment. Using the APTW-IPL for other life–stress relationships that consider other accelerating factors such as temperature and vibration. Another possible investigation derived from what is proposed in this article is to carry out a multivariate model where the stress-strength is measurable. The multivariate analysis is possible given the flexibility of the IPL model and the APT. Finally, a Bayesian perspective can be added to the APTW-IPL with which the parameters of the proposed model can be estimated.

Disclosure statement

No potential conflict of interest was reported by the author(s).

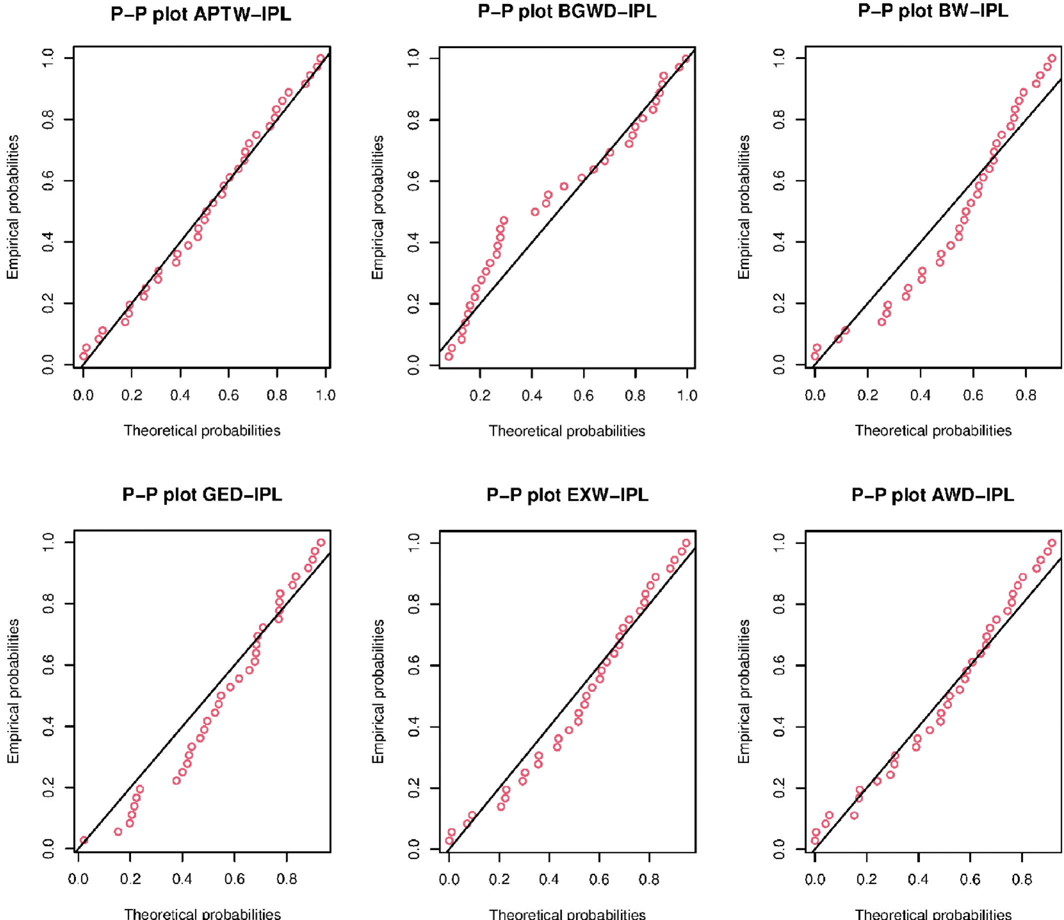

Figure 13. P-P plots for LVDT.

Notes on contributors

Luis Carlos Méndez González Ph.D. is currently a full-time professor at the Department of Industrial Engineering and Manufacturing at the Autonomous University of Ciudad Juárez, México. He received his Ph.D. in Science in Engineering in 2015. He received his M.S in Industrial Engineering from the Technological Institute of Ciudad Juarez in 2011 and his B.S in Electronics Engineering in 2007. He has more than fifteen years in software, hardware design, Applied Statistics, Measurement System Analysis, Reliability Engineering, and Quality Engineering. He is currently a member of the National Researchers System from México as Level 1. His research interests include reliability and degradation modeling, stochastic modeling, hardware, and software design, and Machine Learning.

Luis Alberto Rodríguez-Picón Ph.D. is currently a full-time professor at the Department of Industrial Engineering and Manufacturing at the Autonomous University of Ciudad Juárez, México. He received his Ph.D. in Science in Engineering in 2015. He received his B.S. and M.S. degrees in Industrial Engineering from the Technological Institute of Ciudad Juárez, México, in 2010 and 2012, respectively. He has worked as a professor in industrial engineering, statistics, and mathematics and has several years of professional experience in the automotive industry. He is currently a member of the National Researchers System from México as Level 1. His research interests include reliability and degradation modeling, stochastic modeling, multivariate statistical modeling, and design of experiments.

Iván JC Pérez-Olguín received a Doctor of Science degree in industrial engineering from the Technological Institute of Ciudad Juarez, Mexico. He is currently a full-time Professor and a Researcher with the Autonomous University of Ciudad Juarez, Mexico. He has published in journals, conference proceedings, and books more than 50 articles; he also contributed to the automotive industry with two patents and four utility models. His research interests include robust optimization, reliability tests, product optimization, process optimization, and lean manufacturing.

Luis Asunción Pérez-Dominguez completed a B.Sc. in Industrial Engineering at Instituto Tecnológico de Villahermosa, Tabasco, México in 2000 and M.Sc. degrees in Industrial Engineering from Instituto Tecnológico de Ciudad Juárez, Chihuahua, México, in 2003 respectively. PhD. Science of Engineering, at the Autonomous University of Ciudad Juárez, Chihuahua, México in 2016. Dr. Luis currently is professor-Research in the Universidad Autónoma de Ciudad Juárez. His research interests include multiple criteria decision-making, fuzzy sets applications and continuous improvement tools applied in the manufacturing field. Member of The Canadian Operational Research Society (CORS); Also, member of Society for Industrial and Applied Mathematics (SIAM). He is recognized as Research associated by Ministerio de Ciencia Tecnología e Innovación, Colombia (Ministry of Science Technology and Innovation in Colombia). He is member of Sistema Nacional de Investigadores recognized by CONACYT, México. Dr. Perez also is a member of EURO Working Group on MCDA (EWG-MCDA).

David Luviano-Cruz received the Ph.D. degree in sciences from the Centro de Investigación y de Estudios Avanzados del Instituto Politécnico Nacional (CINVESTAV) using artificial neural networks (ANN) to improve path recognition. He is currently an Active Researcher at the Universidad Autónoma de Ciudad Juárez, where he also performs full-time Professor activities. He has published and published more than 23 scientific works with more than 138 citations. His research interests include optimization using artificial neural network algorithms, Pythagorean fuzzy sets, and machine learning.

ORCID

Luis Carlos Méndez-González http://orcid.org/0000-0002-2533-0036
Luis Alberto Rodríguez-Picón http://orcid.org/0000-0003-2951-2344
Ivan Juan Carlos Pérez-Olguin http://orcid.org/0000-0003-2445-0500
Luis Asunción Pérez-Domínguez http://orcid.org/0000-0003-2541-4595
David Luviano Cruz http://orcid.org/0000-0002-4778-8873

References

Aarset, M. V. (1987). How to identify a bathtub hazard rate. *IEEE Transactions on Reliability*, *36*(1), 106–108. https://doi.org/10.1109/TR.1987.5222310

Ahmad, Z., Elgarhy, M., & Abbas, N. (2018). A new extended alpha power transformed family of distributions: Properties and applications. *Journal of Statistical Modelling: Theory and Applications*, *1*(1), 13–28 doi:jsmta/jsmta.2020.1706.

Ali, S., Ali, S., Shah, I., & Khajavi, A. N. (2019). Reliability analysis for electronic devices using beta generalized Weibull distribution. *Iranian Journal of Science and Technology, Transactions A: Science*, *43*(5), 2501–2514. https://doi.org/10.1007/s40995-019-00730-4

Ali, S., Ali, S., Shah, I., Siddiqui, G. F., Saba, T., & Rehman, A. (2020). Reliability analysis for electronic devices using generalized exponential distribution. *IEEE Access*, *8*, 108629–108644. https://doi.org/10.1109/ACCESS.2020.3000951

Basheer, A. M. (2019). Alpha power inverse Weibull distribution with reliability application. *Journal of Taibah University for Science*, *13*(1), 423–432. https://doi.org/10.1080/16583655.2019.1588488

Bebbington, M., Lai, C.-D., & Zitikis, R. (2007). A flexible Weibull extension. *Reliability Engineering & System Safety*, *92*(6), 719–726. https://doi.org/10.1016/j.ress.2006.03.004

Dey, S., Sharma, V. K., & Mesfioui, M. (2017). A new extension of Weibull distribution with application to lifetime data. *Annals of Data Science*, *4*(1), 31–61. https://doi.org/10.1007/s40745-016-0094-8

Diniz Marinho, P. R., Bourguignon, M., & Barros Dias, C. R. (2016). *Adequacymodel: Adequacy of probabilistic models and general purpose optimization* [Computer software manual]. https://CRAN.Rproject.org/package=AdequacyModelRpackageversion2.0.0

Durrans, S. R. (1992). Distributions of fractional order statistics in hydrology. *Water Resources Research*, *28*(6), 1649–1655. https://doi.org/10.1029/92WR00554

Elbatal, I., Ahmad, Z., Elgarhy, B., & Almarashi, A. (2018). A new alpha power transformed family of distributions: Properties and applications to the Weibull model. *Journal of Nonlinear Science and Applications*, *12*(1), 1–20. https://doi.org/10.22436/jnsa.012.01.01

Gurvich, M., Dibenedetto, A., & Ranade, S. (1997). A new statistical distribution for characterizing the random strength of brittle materials. *Journal of M Aterials Science*, *32*(10), 2559–2564. https://doi.org/10.1023/A:1018594215963

He, Y., Wang, L., He, Z., & Xiao, X. (2016). Modelling infant failure rate of electromechanical products with multilayered quality variations from manufacturing process. *International Journal of Production Research*, *54*(21), 6594–6612. https://doi.org/10.1080/00207543.2016.1154215

He, Y., Zhao, Y., Wei, Y., Zhang, A., & Zhou, D. (2019). Modeling and detecting approach for the change point of electronic product infant failure rate. *Microelectronics Reliability*, *99* 1 , 222–231. https://doi.org/10.1016/j.microrel.2019.06.031

Henningsen, A., & Toomet, O. (2011). maxlik: A package for maximum likelihood estimation in R. *Computational Statistics*, *26*(3), 443–458. http://doi.org/10.1007/s00180-010-0217-1

Hjorth, U. (1980). A reliability distribution with increasing, decreasing, constant and bathtub- shaped failure rates. *Technometrics*, *22*(1), 99–107. https://doi.org/10.2307/1268388

Lai, C.-D., Jones, G., & Xie, M. (2016). Integrated beta model for bathtub-shaped hazard rate data. *Quality Technology & Quantitative Management*, *13*(3), 229–240. https://doi.org/10.1080/16843703.2016.1180028

Lee, C., Famoye, F., & Olumolade, O. (2007). Beta-Weibull distribution: Some properties and applications to censored data. *Journal of Modern Applied Statistical. Methods*, *6*(1), 17 doi:10.22237/jmasm/1177992960.

Lehmann, E. L. (1953). The power of rank tests. *The Annals of Mathematical Statistics*, *24*(1), 23–43. https://doi.org/10.1214/aoms/1177729080

Lu, W., & Chiang, J.-Y. (2018). On some life distributions with flexible failure rate. *Quality Technology & Quantitative Management*, *15*(3), 413–433. https://doi.org/10.1080/16843703.2016.1226596

Mahdavi, A., & Kundu, D. (2017). A new method for generating distributions with an application to exponential distribution. *Communications in Statistics-Theory and Methods*, *46*(13), 6543–6557. https://doi.org/10.1080/03610926.2015.1130839

Mann, N. R., Singpurwalla, N. D., & Schafer, R. E. (1974). *Methods for statistical analysis of reliability and life data* (Wiley).

Mead, M. E., Cordeiro, G. M., Afify, A. Z., & Al Mofleh, H. (2019). The alpha power transformation family: properties and applications. *Pakistan Journal of Statistics and Operation Research*, *15*(3), 525–545. https://doi.org/10.18187/pjsor.v15i3.2969

Méndez-González, L. C., Rodríguez-Picón, L. A., Valles-Rosales, D. J., Alvarado Iniesta, A., & Carreón, A. E. Q. (2019). Reliability analysis using exponentiated Weibull distribution and inverse power law. *Quality and Reliability Engineering International*, *35*(4), 1219–1230. https://doi.org/10.1002/qre.2455

Méndez-González, L. C., Rodríguez-Picón, L. A., Valles-Rosales, D. J., Romero-López, R., & Quezada-Carreón, A. E. (2017). Reliability analysis for electronic devices using beta-Weibull distribution. *Quality and Reliability Engineering International*, *33*(8), 2521–2530. https://doi.org/10.1002/qre.2214

Nadarajah, S., Cordeiro, G. M., & Ortega, E. M. (2013). The exponentiated Weibull distribution: A survey. *Statistical Papers*, *54*(3), 839–877. https://doi.org/10.1007/s00362-012-0466-x

Nassar, M., Afify, A. Z., Dey, S., & Kumar, D. (2018). A new extension of Weibull distribution: Properties and different methods of estimation. *Journal of Computational and Applied Mathematics*, *336*(336), 439–457. https://doi.org/10.1016/j.cam.2017.12.001

Nassar, M., Alzaatreh, A., Abo-Kasem, O., Mead, M., & Mansoor, M. (2018). A new family of generalized distributions based on alpha power transformation with application to cancer data. *Annals of Data Science*, *5*(3), 421–436. https://doi.org/10.1007/s40745-018-0144-5

Nassar, M., Alzaatreh, A., Mead, M., & Abo-Kasem, O. (2017). Alpha power Weibull distribution: Properties and applications. *Communications in Statistics-Theory and Methods*, *46*(20), 10236–10252. https://doi.org/10.1080/03610926.2016.1231816

Ramadan, D., & Magdy, W. (2018). On the alpha-power inverse Weibull distribution. *International Journal of Computer Application*, *181*, 6–12 doi:10.5120/ijca2018917657.

Silva, G. O., Ortega, E. M., & Cordeiro, G. M. (2010). The beta modified Weibull distribution. *Lifetime Data Analysis*, *16*(3), 409–430. https://doi.org/10.1007/s10985-010-9161-1

Xie, M., & Lai, C. D. (1996). Reliability analysis using an additive Weibull model with bathtub- shaped failure rate function. *Reliability Engineering & System Safety*, *52*(1), 87–93. https://doi.org/10.1016/0951-83209500149-2

Xie, M., Tang, Y., & Goh, T. N. (2002). A modified Weibull extension with bathtub-shaped failure rate function. *Reliability Engineering & System Safety*, *76*(3), 279–285. https://doi.org/10.1016/S0951-83200200022-4

Zaizai, N. Y. Y. (2019). Properties and applications of alpha power gamma distribution. *Chinese Journal Of Applied Probability And Statistics*, *35*(4), 331. http://aps.ecnu.edu.cn/EN/abstract/article_9153.shtml

Appendix. Observed fisher matrix elements

Let $\psi = \omega v^{\gamma}$

$$I_{\alpha\alpha} = \theta\rho\left[\frac{1}{(\alpha-1)^2} - \frac{log(\alpha)+1}{\alpha^2 \cdot log^2(\alpha)}\right] - \frac{1}{\alpha^2}\sum_{i=1}^{\theta}\sum_{j=1}^{\rho}\left[1 - e^{-(\psi_i t_{i,j})^{\beta}}\right]$$

$$I_{\alpha\beta} = \frac{1}{\alpha}\cdot\sum_{i=1}^{\theta}\sum_{j=1}^{\rho}\left[(\psi_i t_{i,j})^{\beta}\cdot log(\psi)\cdot e^{-(\psi_i t_{i,j})^{\beta}}\right]$$

$$I_{\alpha\omega} = \frac{\beta}{\alpha\gamma}\cdot\sum_{i=1}^{\theta}\sum_{j=1}^{\rho}\left[(\psi_i t_{i,j})^{\beta}\cdot e^{(-\psi_i t_{i,.j})^{\beta}}\right]$$

$$I_{\alpha\gamma} = \frac{\beta}{\alpha}\cdot\sum_{i=1}^{\theta}\sum_{j=1}^{\rho}\left[(\psi_i t_{i,j})^{\beta}\cdot log(v_i)\cdot e^{-(\psi_i t_{i,j})^{\beta}}\right]$$

$$I_{\beta\alpha} = I_{\alpha\beta}$$

$$I_{\beta\beta} = \frac{\theta\rho}{\beta^2} + \sum_{\iota=1}^{\theta}\left\{\left[log^2\left(\psi_{\iota}\, t_{\iota,j}\right).\left(\psi_{\iota}\, t_{\iota,j}\right)^{\beta}.e^{-\left(\psi_{\iota}\, t_{\iota,j}\right)^{\beta}}\right].\left(log\,(\alpha).\left(\psi_{\iota}\, t_{\iota,j}\right)^{\beta} - log\,(\alpha)\right)\right\} - \sum_{\iota=1}^{\theta}\sum_{j=1}^{\rho}\left[\left(\psi_{\iota}\, t_{\iota,j}\right)^{\beta}.\, log^2\left(\psi_{\iota}\, t_{\iota,j}\right)\right]$$

$$I_{\beta\omega} = \frac{\omega\rho}{\theta} - \frac{1}{\theta}\sum_{i=1}^{\theta}\sum_{j=1}^{\rho}\left[(\psi_i t_{i,j})^{\beta}\right] - \frac{1}{\omega}\sum_{i=1}^{\theta}\sum_{j=1}^{\rho}\left[(\psi_i t_{i,j})^{\beta}\cdot log(\psi_i t_{i,j})\cdot\left\{\beta + log(\alpha)e^{-(\psi_i t_{i,j})^{\beta}}\right\}\right] + \sum_{i=1}^{\theta}\sum_{j=1}^{\rho}\left[(\psi_i t_{i,j})^{\beta}\cdot log(\psi_i t_{i,j})e^{-(\psi_i t_{i,j})^{\beta}}\cdot\left\{-\frac{\beta log(\alpha)}{\omega}\cdot\left((\psi_i t_{i,j})^{\beta} - 1\right)\right\}\right]$$

$$I_{\beta\gamma} = \sum_{i=1}^{\theta}[log(v_i)] - \sum_{i=1}^{\theta}\sum_{j=1}^{\rho}\left[(\psi_i t_{i,j})^{\beta} log(v_i)\cdot\left(\beta log(\psi_i t_{i,j}) + 1\right)\right] + log(\alpha)\sum_{i=1}^{\theta}\sum_{j=1}^{\rho}\left[log(v_i)e^{-(\psi_i t_{i,j})^{\beta}} \cdot\left\{(\psi_i t_{i,j})^{\beta}\beta log(\psi_i t_{i,j}) - (\psi_i t_{i,j})^{2\beta}\beta log(\psi_i t_{i,j}) + (\psi_i t_{i,j})^{\beta}\right\}\right]$$

$$I_{\omega\alpha} = I_{\alpha\gamma}$$

$$I_{\omega\beta} = I_{\beta\omega}$$

$$I_{\omega\omega} = -\frac{\theta\beta\rho}{\omega^2}\cdot\sum_{i=1}^{\theta}\sum_{j=1}^{\rho}\left[(\psi_i t_{i,j})^{\beta}\left(\frac{\beta(\beta-1)}{\omega^2}\right)\right] + \frac{log(\alpha)}{\omega^2}\cdot\sum_{i=1}^{\theta}\sum_{j=1}^{\rho}\left[(\psi_i t_{i,j})^{\beta}e^{-(\psi_i t_{i,j})^{\beta}}\cdot\left\{\beta(\beta-\beta(\psi_i t_{i,j})^{\beta}-1)\right\}\right]$$

$$I_{\omega\gamma} = \frac{\beta^2}{\omega}\cdot\sum_{i=1}^{\theta}\sum_{j=1}^{\rho}\left[log(v_i)\cdot\left\{log(\alpha)(\psi_i t_{i,j})^{\beta}e^{(-\psi_i t_{i,j})^{\beta}} - log(\alpha)(\psi_i t_{i,j})^{2\beta}e^{-(\psi_i t_{i,j})^{\beta}} - (\psi_i t_{i,j})^{\beta}\right\}\right]$$

$$I_{\gamma\alpha} = I_{\alpha\gamma}$$

$$I_{\gamma\beta} = I_{\beta\gamma}$$

$$I_{\gamma\omega} = I_{\omega\gamma}$$

$$I_{\gamma\gamma} = \beta\left\{\sum_{i=1}^{\theta}\sum_{j=1}^{\rho}\left[-log^2(v_i)\beta(\psi_i t_{i,j})^{\beta}\cdot\left(log(\alpha)(\psi_i t_{i,j})^{\beta}e^{-(\psi_i t_{i,j})^{\beta}} - log(\alpha)e^{-(\psi_i t_{i,j})^{\beta}}+1\right)\right]\right\}$$

.